FROM SINGLE BUBBLES ON SOLID SURFACES TO MASSIVE BUBBLY FLOWS DURING DECOMPRESSION SICKNESS

T.D. Karapantsios, M. Kostoglou, S.P. Evgenidis

Division of Chemical Technology, Department of Chemistry, Aristotle University of Thessaloniki, Univ.Box 116, 54124, Thessaloniki, Greece, Email:karapant@chem.auth.gr, kostoglu@chem.auth.gr, sevgenid@chem.auth.gr

ABSTRACT

Gas bubbles can be generated on solid surfaces covered by a liquid as a result of desorption of dissolved gases when the liquid becomes supersaturated with respect to dissolved gases.

This work starts from basic phenomena controlling single bubble growth on a solid surface, extends to growth of multiple adjacent bubbles and their subsequent detachment from the surface into the liquid and, finally, copes with the detection and characterization of multiple bubbles flowing with the liquid (bubbly flow). Apparently, this is a very broad topic and can not be dealt with in just one report.

As regards bubble growth, here only the case of thermal degassing is examined in which bubbles are produced locally on a hot spot surrounded by cold liquid layers. Thermal degassing is more general than decompression degassing (in fact, it encompasses it) since in addition to mass transfer involves also heat transfer processes.

As regards bubbly flows the emphasis is on novel techniques that allow measurement of gas/liquid fractions and bubble size distributions at conditions such as those met during Decompression Sickness (DCS) in human veins and arteries.

1. INTRODUCTION

Decompression sickness (DCS) is a clinical syndrome caused by rapid reduction of environmental pressure in the body that results in formation of bubbles within body tissues. In current space programs there is a risk of hypobaric DCS during extravehicular activities (EVA) because in that case crewmembers go from a cabin pressure of 14.7 psia inside the space shuttle or international space station (ISS) to the space suit pressure of 4.3 psia (http://spaceflight.nasa.gov). The fact is that there has been less DCS occurrence during EVAs than statistically expected chiefly due to the 100% oxygen prebreathe and the slow depressurization protocol followed by astronauts [1].

EVA preparation protocols are designed in order to prevent serious DCS symptoms, and are based on statistical evaluation of previous decompression experiments. Although up to now no serious DCS symptoms have occurred, these preparation protocols cannot assure the safety of crewmembers performing EVAs due to the big variation of individual and day-by-day susceptibility but also due to the multiple factors affecting DCS occurrence. Furthermore, it is not known if these protocols can be efficient for populations on which little data exist such as women, previously injured people, etc. In addition, the long time needed for EVA preparations makes it almost impossible for astronauts to use it in emergency situations [2]. All the above together with the increasing need for EVAs in the following years, underline the importance of understanding the physical mechanisms controlling the formation of bubbles in the human body and also developing in-vivo non-intrusive techniques for their detection.

This work aims to make the connection between liquid degassing (bubble growth and detachment) and bubbly flow which is essentially the precursor of DCS. In order to develop techniques for real-time identification of bubbles in the blood flow and tissues, it is important to understand bubble growth behaviour and bubbles interaction when growing in proximity. In the present study the research performed in our laboratory on understanding bubble growth and detachment dynamics during thermal degassing and on bubbly flow identification techniques namely an electrical one and an acoustical one, is presented.

2. BUBBLE GROWTH STUDY

The traditional way to study bubble generation and growth due to the oversaturation of a liquid with respect to a dissolved gas (degassing) is through the application of a sudden decompression to the liquid. In such experimental studies the visual observation of an isolated growing bubble is difficult chiefly because bubbles are generated in large numbers in the bulk of the liquid whereas convective currents induced by decompression drift the developing bubbles away from their nucleation sites.

To overcome this problem an experimental design has been proposed which admits the generation of just a single bubble in the liquid. This is realized by using a miniature spherical heater submerged in the bulk of the liquid. The heater is suddenly heated and as the liquid becomes locally supersaturated with respect to the dissolved gas, a bubble forms at the surface of the thermistor. Subsequently, the bubble grows with transfer of mass of the dissolved gas from the bulk of the liquid to the bubble surface.

In a series of ESA (European Space Agency) Parabolic Flight Campaigns, we exploited the low-g conditions achieved during the free-fall of an airplane to study the bubble dynamics during degassing of several liquids. Microgravity conditions are necessary for eliminating the effects of bubble buoyancy and natural convection

in order to obtain results amenable to rigorous theoretical interpretation.

The experimental set up is described in detail elsewhere [3]. The core of the equipment is an ultra-precision thermostat unit into which an exchangeable sample cell unit can be inserted. Bubbles are growing on the surface of a small, axisymmetrical, glass-coated, NTC thermistor (Thermometrics, Inc. R=0.125 mm) serving as a local heater. Bubble images from this heater are recorded by a CCD color camera and analyzed by a custom software.

Continuous heat pulses of constant power are applied to the heater through a special circuitry. The power of the pulses is constant through each run but varies among runs. Registering the voltage drop across the heater allows the delivered power and temperature of the heater to be estimated. Here, results concerning only PBS (Phosphate Buffer Saline), a common blood substitute for lab work, are presented. For experimental convenience CO_2 is selected as the desorbing gas due to its high solubility to liquids.

2.1 Single bubble growth

A detailed mathematical description of the process includes the solution of transient heat and mass transfer equations in the gas and liquid phases (3-dimensional geometry) along with the appropriate boundary conditions on the surface of the bubble and the heater [4]. The problem includes a moving boundary with the motion being part of the solution. In addition, the very high temperature gradient along the surface of the bubble induces a Marangoni motion which transfers hot fluid from the heater to the remote parts of the bubble surface, tending to equilibrate bubble and heater temperatures.

An initial attempt to simulate the problem of bubble growth on the thermistor was based on a spherically symmetric (1-D) model of a spherical bubble growing at a constant temperature (equal to the steady state heater temperature) and a far field temperature equal to the initial bulk liquid temperature. The problem was solved using a well known similarity transformation [5] and has lead to a power law relation between bubble radius and time with an exponent value equal to 0.5. However, the corresponding experimental curves [3] were best-fitted by lower (than 0.5) exponent values [6].

A next step was to approximate the problem by a 1-D model but now the assumption is that the bubble grows at a uniform but time dependent temperature [7]. This temperature equals the instantaneous value of the average temperature across the whole bubble. Of course, the evolution of the average bubble temperature is not known (its computation requires the knowledge of the complete flow field) but based on the above 1-D model an inverse problem can be formulated: To which bubble average temperature evolution profiles, the observed bubble growth curves correspond? Comparing the evolution of bubble temperature estimated from experimental growth curves with the measured temperature of the heater reveals important information for the phenomena dictating bubble growth. Two typical experimental growth curves for single bubbles grown in PBS obtained during parabolic flights are shown in Fig. 1. In the legend of the Figure there is the code number of the experiment, the supplied heat flux and the min/max temperatures of the heater measured during the bubble growth process. Theoretical results are given as dotted lines. The success of the fitting (by adjusting the evolution of the unknown bubble temperature) of the theoretical to experimental curves is described through the correlation coefficient R^2. Apparently, bubbles grow faster as the heat flux increases.

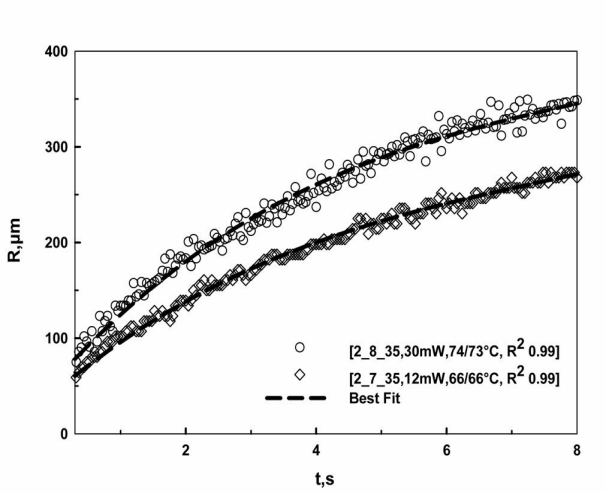

Fig. 1. Evolution of the radius of single bubbles for two different values of the heat flux supplied by the heater.

2.2 Multiple bubble growth and detachment

For low power heat pulses, single bubbles are observed to grow always at the same location of the heater for the entire heating period, a situation indicating heterogeneous nucleation. At higher power levels, two or more bubbles are noticed to grow simultaneously at different (but always the same) locations on the heater's surface indicating once more heterogeneous nucleation [8]. Such a group of simultaneous bubbles (designating a *bubble generation*) grows for less time than single bubbles do and then detaches thus allowing for more bubble generations to appear during the same heating period. The number of simultaneous bubbles per generation as well as the number of generations within the same heating period increase with power level. The evolution of bubbles size -up to detachment- of several generations (G) of bubbles is shown in Fig. 2.

Simultaneous bubbles emerging at different sites of the heater do not grow at exactly the same rate. Using the previous 1-D model to estimate the average bubble temperature from the experimentally obtained bubble radius reveals that simultaneous bubbles do not grow isothermally to each other, apart from a short period at

the beginning of heating when they are smaller than the size of the heater. This is attributed to local deviations of the heater geometry from sphericity: bubbles with lower temperatures grow at higher-curvature regions. In addition, the temperature of bubbles progressively diverges from the heater's temperature. This behavior is ascribed to the onset of Marangoni convection around the growing bubbles.

Careful comparisons reveal that multiple bubbles grow at lower rates than single bubbles at equivalent thermal conditions, a fact which implies that multiple bubbles growing in proximity can deplete the dissolved gas in their neighbourhood. The competition of adjacent bubbles for the available dissolved gas is further supported by the observed thermal saturation limit (temperature above which any increase in temperature has no effect on growth rate) for multiple bubbles which is distinctly lower than that for single bubbles.

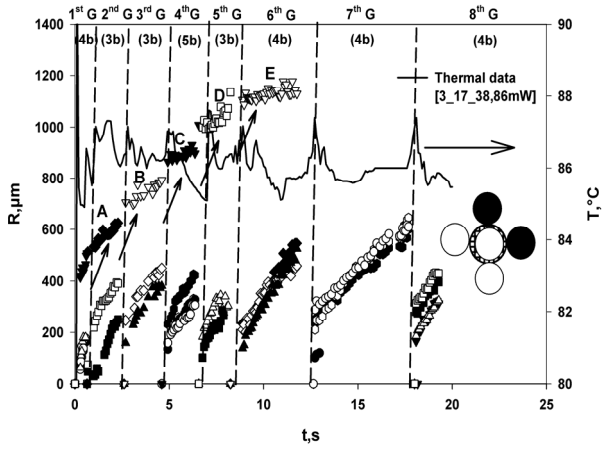

Fig. 2. Multiple bubble growth evolution curves (radius vs time) and heater temperature data. The location of nucleation sites is shown schematically by the circles in the insert.

Multiple bubbles detach at some point along their growth due to g-jitters. Interestingly, they detach synchronously to each other and at much smaller sizes than single bubbles do. This is attributed to the higher temperatures employed to produce multiple bubbles which are capable of destabilizing the contact line of the bubbles with the heater.

3. BUBBLY FLOWS

Once multiple bubbles detach from their nucleation sites they form a bubble cloud which can be dragged by a liquid stream if flow conditions are imposed e.g., in blood stream. Thus, it is easy to realize that detecting and sizing bubbles intravascularly may indicate DCS severity in humans. Given that the traditional Doppler bubble detection technique can offer only limited information, [9], we have made a serious effort over the last five years to examine theoretically and measure experimentally the behaviour of such bubble cloud and its interaction with the liquid flow.

3.1 Computational Fluid Dynamics (CFD)

The commercial CFD code Fluent was used to simulate the pulsating two-phase blood/bubble flow. Initial simulations were performed inside a simplified 2-D axisymmetric vertical column having the diameter of human vena cava (21mm) in order to provide basic insight to the problem. The importance of bubble size in interacting with the bulk flow is evident in the representative results of Fig. 3. The 30μm bubbles completely follow the motion of the bulk liquid leading to a uniform air volume fraction whereas the 300μm bubbles diverge from the liquid flow field due to their inertia and buoyancy leading to a non-uniform concentration profile both in the radial and axial directions.

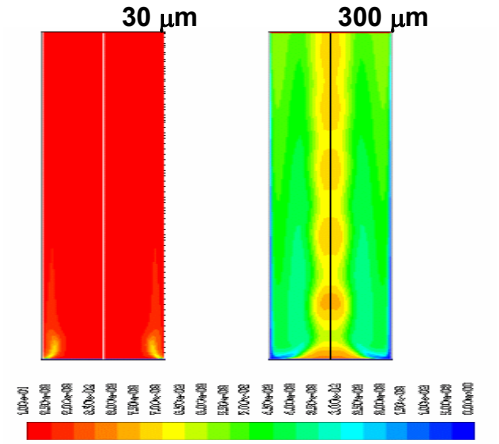

Fig. 3. Contours of air volume fraction for pulsating flow 0.6Lit/min, pulsation 60 bpm, 50% pulse amplitude, 10% air volume fraction.

Simulations were also conducted in a 3D representative geometry of an artery (Fig. 4), obtained from [10].

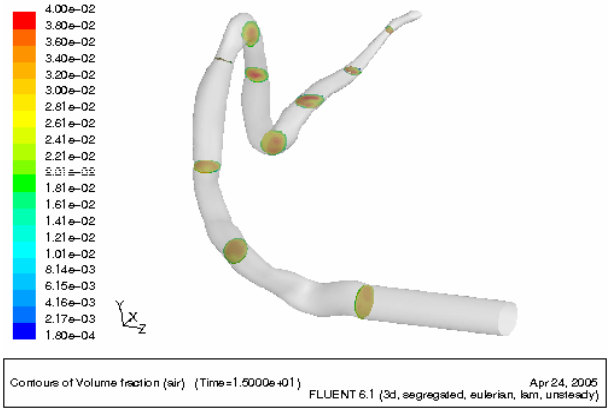

Fig. 4. Contours of air volume fraction for pulsating flow 0.6Lit/min, artery length 500 mm and diameter 5-20 mm, pulsation 60 bpm, 50% pulse amplitude, 3% air volume fraction. The picture refers to 300 μm bubbles.

It is evident that for 300 μm bubbles the 3D sharp turns along with the diameter expansions/contractions yield air concentration non uniformities also in the angular direction which complicate further the flow.

3.2 Experimental bubble detection and sizing

We have developed an electrical impedance tomography (ERT) technique for registering the temporal distribution of the gas and liquid phases during bubbly flows based on the different electrical properties of the two phases. In order to obtain such information a strategic selection of probe geometry and the corresponding algorithm for signal interpretation have been developed. Fig. 5 shows indicative electrical signals from benchtop experiments on a PMMA tube having the size of vena cava (21 mm). The effect of bubble size is evident. Frequency component analysis (Fourier Transform) of such signals yields quantitative results regarding average gas concentration and bubble size.

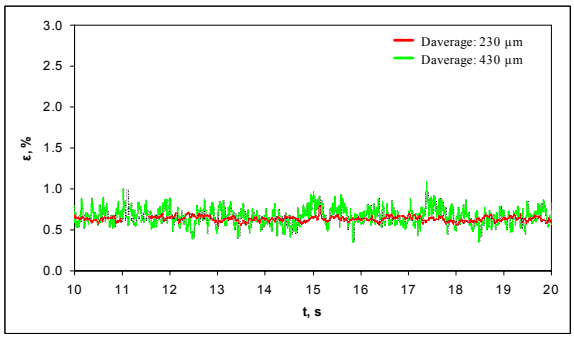

Fig. 5. Gas concentration (ε) electrical signals for bubble clouds with average diameters: 230 and 430 μm.

We have also developed an acoustic spectroscopy (AS) technique for bubble detection and sizing. The attenuation of the ultrasound signal and the alteration of the phase velocity due to bubble presence in the liquid are employed in the signal reduction algorithm to give a measure of the quantity of bubbles and bubble size distribution. Fig. 6 presents typical ultrasound attenuation results obtained at the same benchtop setup as with ERT.

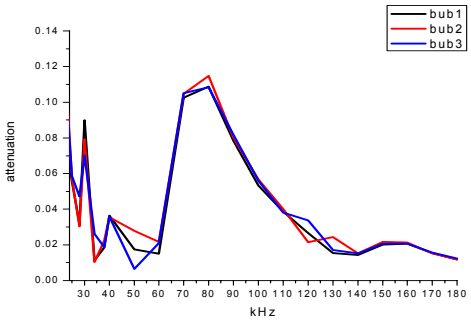

Fig. 6. Ultrasound attenuation with respect to excitation frequency for a gas concentration of 1%.

So far, results from both techniques are promising as they show exceptional sensitivity to variations in both gas fraction and bubble size and agree reasonably with bubble sizes obtained from high resolution optical images, e.g. Fig. 7.

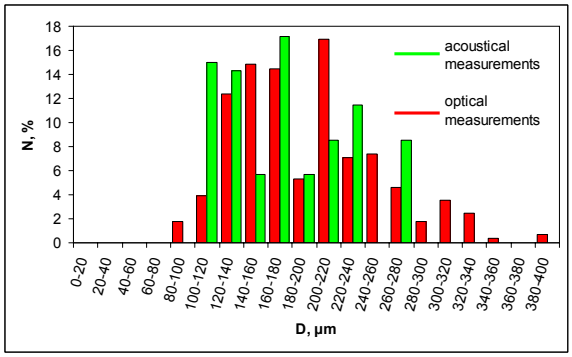

Fig. 7. Comparison between acoustic and optical results (% vs diameter) for a gas concentration 1%.

Funded by an ESA/GSTP project we are currently making preparations for doing tests on anesthetized swines. Of course, the final and more important validation tests will come next on humans.

4. REFERENCES

1. Powell M., et al. Modifications of Physiological Processes Concerning Extravehicular Activity in Microgravity, *24th International Conference on Environmental Systems and 5th European Symposium on Space Environmental Control Systems* Friedrichshafen, Germany, June 20-23, 1994.
2. Lango T., et al. Diffusion Coefficients for Gases in Biological Fluids: a Review, *Undersea Hyperbaric Medicine*, Vol. 23, 247-272, 1996.
3. Divinis, N., et al. Bubbles Growing in Supersaturated Solutions at Reduced Gravity, *AIChE J.*, Vol. 50, 2369-2382, 2004.
4. Kostoglou M. and Karapantsios T.D., Bubble Dynamics During the Nonisothermal Degassing of Liquids. Exploiting Microgravity Conditions, *Advances in Colloid and Interface Science*, Vol.134-135, 125-137, 2007.
5. Divinis, N., et al. Self-similar Growth of a Gas Bubble Induced by Localized Heating: the Effect of Temperature-Dependent Transport Properties, *Chemical Engineering Science*, Vol. 60, 1673-1683, 2005.
6. Kostoglou M. and Karapantsios T.D., Approximate Solution for a Nonisothermal Gas Bubble Growth over a Spherical Heating Element, *Industrial Engineering Chemistry Research*, Vol. 44, 8127-8135, 2005.
7. Divinis N., et al. Bubble Dynamics During Degassing of Dissolved Gas Saturated Solutions at Microgravity Conditions, *AIChE J.*, Vol. 52, 3029-3040, 2006.
8. Karapantsios T., et al. Nucleation, Growth and Detachment of Neighboring Bubbles over Miniature Heaters, *Chemical Engineering Science*, Vol. 63, 3438-3448, 2008.
9. Hills B. A. and Grulke D. C., Evaluation of Ultrasonic Bubble Detectors in vitro Using Microbubbles at Selected Velocities, *Ultrasonics*, Vol.13, 181-184, 1975.
10. Berthier B., et al. Blood Flow Patterns in an Anatomically Realistic Coronary Vessel: Influence of 3 Different Reconstruction Methods, *J. Biomechanics*, Vol. 35, 1347-1356, 2002.

Acknowledgment

We are grateful to ESA for the parabolic flight campaigns where we studied bubble growth dynamics and also for the GSTP projects aiming to develop an in-vivo embolic detector for humans.